

EUROPEAN ORGANIZATION FOR NUCLEAR RESEARCH  
CERN — SL DIVISION

SL-Note-2001-023 HRF

CERN Nufact Note 082

# Control Instabilities in a Pulsed Multi-Cavity RF System with Vector Sum Feedback (A Mathematical Analysis)

**J. Tückmantel**

## Abstract

Upcoming projects relying on pulsed linear accelerators intend to use superconducting RF systems. Cost reasons suggest driving several cavities by a common transmitter, controlled over a vector sum feedback system, possibly supported by a feed forward system. Numerical simulations hint that such a system may become uncontrollable under certain conditions. In the present paper, for a model very close to reality, we will present a mathematical proof that in fact spontaneous symmetry breaking is possible for these configurations, defining also the precise conditions under which it will take place. These can be used as an estimate for the real RF system stability limits. The listing of a small program demonstrating the mechanism numerically for two cavities is attached.

Geneva, Switzerland  
31 May, 2001

open-2001-052  
31/05/2001



## 1 INTRODUCTION

When raising the field in a cavity, the Lorentz force will slightly deform its shape and thus change its resonance frequency. If the system bandwidth is small and fields are high – as generally is the case in systems applying superconducting cavities – this frequency change can lead to considerable voltage deviations. When the RF system is pulsed, the cavity is excited to mechanical oscillations and the tuner can only compensate the corresponding average detuning, but fast dynamic detuning remains. Therefore a RF vector feedback correcting for these changes controls the transmitter.

In numerical simulations with ‘SPLinac’ [1], this mechanism always works well provided that there is only *one* cavity controlled by the vector feedback. However, when we supply *several* cavities by the same transmitter, controlled by the vector *sum* feedback, control instabilities showed up under certain circumstances, see e.g. Appendix A. Based on a model, we will analyse these instabilities mathematically in this paper.

For one cavity per transmitter the vector feedback perfectly controls the unique cavity voltage. For more than one cavity driven by a single transmitter the vector sum feedback still controls the *sum* voltage but has no influence at all on the other degrees of freedom of the system, i.e. how cavities share the sum amongst each other. For identical static cavity parameters intuitively (without justification) we assume that cavities equitably share the voltage. However, as we shall demonstrate in this paper, this assumption is not always true; spontaneous symmetry breaking may take place.

Imagine two cavities driven by a common transmitter with all static settings (as static detuning,  $Q_{\text{ext}}$ , power splitting, vector sum contribution) perfectly identical for both cavities. Let us assume now that by a small initial perturbation (noise) both cavities have a microscopically small mutual difference in RF tune. Hence, due to the common transmitter, cavity fields are not identical while the RF is on. The vector sum feedback will immediately adjust the drive to obtain a perfect vector sum, so one cavity will have a deviation  $+dV$ , the other one  $-dV$  with respect to the nominal voltage. Hence the created Lorentz force ‘kick’ for the two cavities will slightly differ and hence also the additionally excited mechanical oscillation amplitudes. This mechanism enforces that at the next pulse again a tune difference between the two cavities exists. Now it cannot be excluded that the tune deviation so created is larger than the initial deviation and is thus amplified from pulse to pulse to macroscopic size.

We will mathematically analyse this mechanism and establish the precise stability limits for the chosen simplified model. As we shall see in the numerical examples, the mathematical predictions and the simulation with ‘SPLinac’ agree quite well. Therefore the effect observed with ‘SPLinac’ is not a computer artefact – always a justified doubt when a computer tells us things not initially expected – but has to be taken seriously.

## 2 THE MODEL

Precise behaviour with many system parameters can only be simulated numerically, but we want to understand the mechanism and estimate the essential parameter combinations. Therefore we have to simplify in an intelligent way, not sacrificing essential ingredients.

The first simplification is the use of a ‘rectangular’ RF pulse, i.e. the cavity field rises instantly from zero to its design field and at the end drops instantly to zero again. Generally the ‘RF on time’ is short compared to the mechanical cavity oscillation period. Therefore we will even use the limit of a short RF pulse length (‘delta function excitation’) where Lorentz force and ‘RF on time’ enter as a product only. Practically this means that we do not take into account the precise shape of cavity loading and unloading but use an effective Lorentz force averaged over the ‘RF on time’.

The second simplification is the application of a *perfect* RF vector sum feedback with infinite gain and without delays. Practically this means that there are no voltage over- or undershoots and no residual errors, the vector sum is always perfect.

We will write down as a first step the general formula predicting the mechanical and voltage amplitudes of the next pulse from the quantities of the previous one. Then we will determine the equilibrium point, where the previous and following amplitudes are mathematically identical. This is

the point where we expect the system to settle after an initial transient of a few linac pulses.

Finally we will derive in linear approximation how an initial perturbation around this equilibrium will propagate from pulse to pulse. The eigenvalues of the corresponding matrix equation will predict the parameter settings for stability or instability.

The author has also programmed these formulas and checked that the matrix equation shows exactly the same output as the formula generally valid (for small deviations from the equilibrium). A listing of the (very short) program with the *generally valid* formula is given in Appendix C such that the ‘unfaithful’ can check and run the program and see stability or instability according to small parameter changes. The outcome can be predicted beforehand by inspecting the main eigenvalue, calculated according to the formula (39) we will derive here, i.e. there is a perfect agreement.

Also, numerical outputs from this program are shown in Appendix D for a typical example, comparing two nearly identical settings, one stable – with an absolute eigenvalue slightly below unity – the other unstable – with an absolute eigenvalue slightly above unity.

## 2.1 The Mechanical cavity movement

We assume a mechanical resonator excited by a constant force between 0 and  $T_1$  (‘RF on’) and oscillating free from  $T_1$  to the linac repetition time  $T$  (‘RF off’):

$$(1) \quad \ddot{s} + 2\sigma \dot{s} + \omega_{mech}^2 s = \begin{cases} \omega_{mech}^2 F & 0 \leq t \leq T_1 \\ 0 & T_1 \leq t \leq T \end{cases}$$

with the mechanical resonance  $\omega_{mech}$  and attenuation  $\sigma = \omega_{mech} / (2Q_{mech})$ . This equation of motion is compatible with an additional free oscillation (homogeneous solution) of any amplitude  $s_0$  – remainder of the previous pulses. We use complex notation with  $s$  proportional  $\exp(i\bar{\omega}t)$ ; the real part of  $s$  represents the observed movement, the imaginary part being proportional to the velocity. The free oscillation frequency  $\bar{\omega}$  is determined by the resonance condition  $\omega_{mech}^2 - \bar{\omega}^2 + 2i\sigma\bar{\omega} = 0$ .  $\bar{\omega}$  contains the attenuation as the imaginary part and can – for small attenuation – be approximated by  $\bar{\omega} \approx \omega_{mech} + i\sigma$ . The movement (inhomogeneous solution)

$$(2) \quad s_{inh}(t) = F(1 - \exp(i\bar{\omega}t))$$

solves the equation of motion in  $0 \leq t \leq T_1$  and, having the boundary condition  $s(0)=0$ , it fulfils the continuity condition at  $t=0$ . This movement becomes at  $t=T_1$ , where  $F$  drops to zero, an additional free oscillation with the same amplitude to obey continuity of location ( $\text{Re}(s)$ ) and velocity ( $\text{Im}(s)$ ). Therefore in the range  $T_1 < t \leq T$  we get the solution.

$$(3) \quad s(t) = F(1 - \exp(i\bar{\omega}T_1))\exp(i\bar{\omega}(t - T_1)) + s_0 \exp(i\bar{\omega}t)$$

Fig. 1 shows the equilibrium oscillation pattern for different duty-cycles  $T_1/T$  with constant product  $T_1 F = 1$  including the ‘delta’ case where  $T_1 \rightarrow 0$  and  $F \rightarrow \infty$ . Fig. 2 illustrates the cavity momentum. We see the momentum transfer (‘kick’) during the ‘RF on time’, especially the instantaneous ‘delta-kick’.

For a ‘RF on time’  $T_1$  short compared to a mechanical oscillation (3) can be approximated by a delta-kick excitation (see fig. 1)

$$(4) \quad s(t) = (s_0 - i\bar{\omega}T_1 F) \exp(i\bar{\omega}t)$$

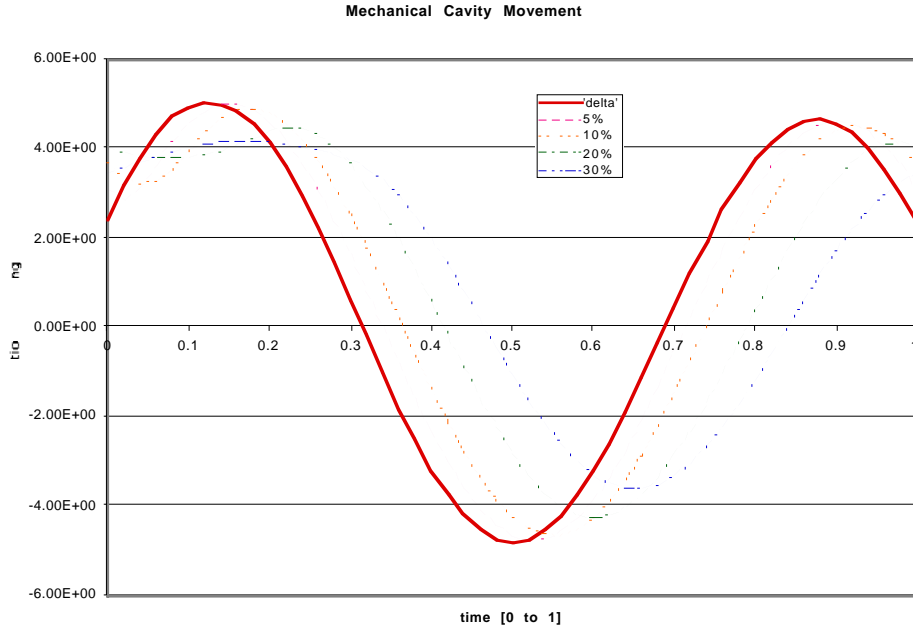


Fig. 1: The mechanical cavity movement (repetitive equilibrium) with finite length of 'RF on' period for a 'duty cycle  $T_1/T$ ' of 30%, 20%, 10% and 5% while conserving  $T_1 F = 1$ . For the 'delta' case the limit  $T_1 \rightarrow 0$  and  $F \rightarrow \infty$  is shown.

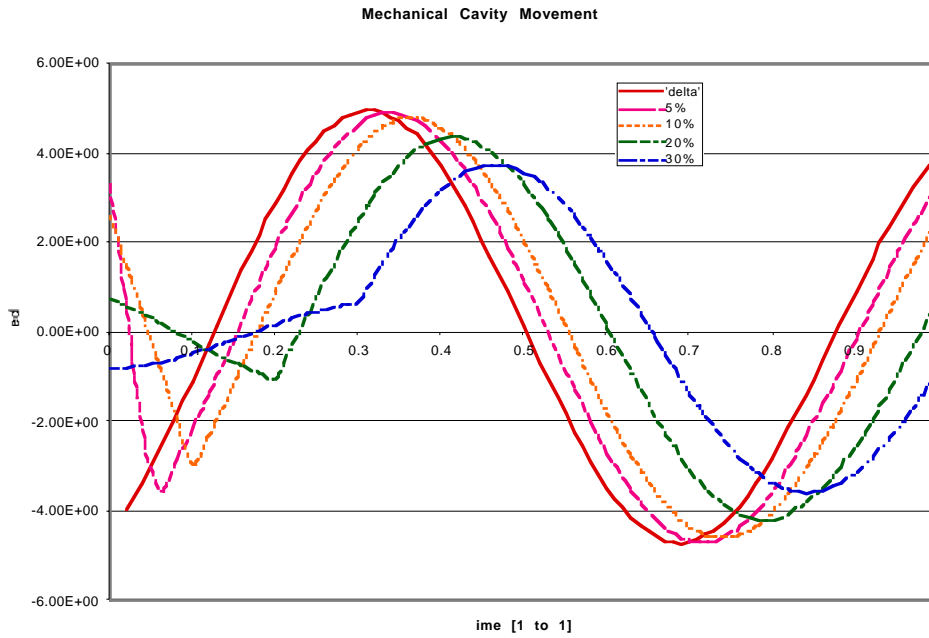


Fig. 2: As Fig. 1 but showing the mechanical speed/momentum of the cavity.

We see that the parameters  $T_1$  and  $F$  no longer enter the problem individually, but only their product.  $s_0$  is the amplitude of the residual free oscillation caused by the previous pulses at  $t=0^-$ , just before receiving the ‘Lorentz kick’.  $s(T)$  is therefore the similar amplitude just before the next ‘Lorentz kick’ at  $t=T^-$ . We get therefore the recursion relation from the ‘old’ mechanical amplitude  $s_0=A_{old}$  to  $s_1=A_{new}$  by

$$(5) \quad A_{new} = (A_{old} - i(\omega T_1 F)_{old}) \rho$$

with the complex ‘transfer factor’  $\rho$  for one linac repetition time  $T$

$$(6) \quad \rho = \exp(i\omega T) = |\rho| (\cos(\psi) + i \sin(\psi))$$

$$(6a) \quad \psi = 2\pi(f_{mech} / f_{rep})$$

$$(6b) \quad |\rho| = \exp\left(-\pi (f_{mech} / f_{rep}) / Q_{mech}\right)$$

In fact,  $|\rho|$  is the damping factor of the mechanical oscillation during the repetition time  $T=1/f_{rep}$  and  $\psi$  the mechanical phase advance during the same interval. We have indexed the expression  $(\omega T_1 F)$  by ‘old’ since  $F$  may vary from pulse to pulse.

### 2.1.1 The equivalent tune change

Until now we have only talked about mechanical movement. For small mechanical amplitudes this movement is proportional to the cavity detuning with respect to its *relaxed* tune status. Therefore we can interpret the above equations also for the detuning. To keep the formula as simple as possible, we will not use the detuning expressed in Hz but in bandwidths  $B$  of the corresponding cavity-transmitter system. We thus write the cavity detuning as complex variable  $z$  – in fact the real part of  $z$  is the actual detuning – repeating (1) as

$$(7) \quad \ddot{z} + 2\sigma\dot{z} + \omega_o^2 z = \begin{cases} \omega_o^2 F & 0 \leq t \leq T_1 \\ 0 & T_1 < t < T \end{cases}$$

If in (7) we apply  $F$  forever (i.e.  $T_1 \rightarrow \infty$ ),  $\dot{z}$  and  $\ddot{z}$  will decay to zero and we will end up with the static detuning under Lorentz force  $z_\infty \equiv F$ . For a given constant cavity excitation we know to express  $z_\infty$  using the Lorentz detuning constant  $k_L$  and the cavity field. Therefore we can immediately express the detuning, measured in bandwidths, by

$$(8) \quad F = z_\infty = k_L E^2 / B = k_L V^2 / (L^2 B)$$

where  $E$  is the cavity field,  $V$  its voltage and  $L$  the nominal cavity length. We can thus define the ‘Lorentz kick’  $K_{old}$  as a function of the cavity voltage  $V_{old}$

$$(9) \quad K_{old} = \omega_{mech} T_1 F_{old} = |V_{old}|^2 \omega_{mech} T_1 k_L / (L^2 B) = K_0 |V_{old}|^2 / V_0^2$$

with the nominal (real) voltage  $V_0$  and the nominal ‘Lorentz kick’  $K_0$  defined as

$$(10) \quad K_0 = k_L V_0^2 \omega_{mech} T_1 / (L^2 B) = k_L E_0^2 \omega_{mech} T_1 / B$$

and get the pulse to pulse recursion relation for the detuning equivalent to (5)

$$(11) \quad z_{new} = (z_{old} - i K_0 |V_{old}|^2 / V_0^2) \rho$$

The actual detuning (in bandwidths) is  $\text{Re}(z)$ .

## 2.2 The tune dependent cavity voltage with constant generator

A cavity driven by a constant generator, has a steady state voltage amplitude proportional to

$$(12) \quad V \propto \frac{1}{1 - i 2\Delta f / B}$$

where  $\Delta f$  is the cavity detuning with respect to the generator frequency and  $B$  is the system band width. Since the RF feedback is assumed to have very high (infinite) gain, there are negligible (no) transients when switching the field on, thus only the steady state exists. The detuning  $\Delta f$  has two components, one being the dynamic Lorentz detuning expressed by  $\text{Re}(z)$  (measured in bandwidths) as shown before. Furthermore generally a *static pre-tuning*  $x_{\text{tune}}$  – also expressed in bandwidths – will be applied due to operational considerations. It is set such that the oscillating cavity RF frequency approaches about the generator frequency when ‘RF on’ is required, thus avoiding excess RF power. This pre-tuning has to be considered constant since the tuner is too slow to make any sensitive changes on the time-scale considered. We assume that all cavities have the *same* static detuning  $x_{\text{tune}}$  (real parameter).

Therefore the voltage  $V_n$  of cavity  $n$  for constant generator can be expressed with a constant  $G$ , *unique* for all cavities, as

$$(13) \quad V_n = \frac{G}{1 - i 2(x_{\text{tune}} + \text{Re}(z_n))}$$

## 2.3 The Vector Sum Feedback

The voltages expressed by (13) are added up as vectors (complex numbers) in the RF vector sum device and the generator drive  $G$  is adjusted *instantly* by the feedback such that the average cavity voltage is identical to the nominal cavity voltage  $V_0$ . This enforces for  $N$  supplied cavities the constraint

$$(14) \quad \sum_{n=1}^{n=N} V_n = N V_0 \Rightarrow V_0 = \frac{G}{N} \sum_{n=1}^N \frac{1}{1 - i 2(x_{\text{tune}} + \text{Re}(z_n))}$$

fixing  $G$  and determining uniquely the voltages (13).

## 2.4 Pulsing the system

Following the most probable real operation, we may start with all cavities without oscillation, thus the amplitudes are all equal to zero  $z_{n,\text{old}}=0$ . However, there is no reason not to start with *any* other set  $z_{n,\text{old}}$ .

Starting with the chosen set of  $z_n$ , equations (13) and (14) determine the cavity voltages  $V_n$  as they are forced by the vector sum feedback during ‘RF on’, to obtain the perfect sum voltage. These voltages will produce a ‘Lorentz kick’ and equation (11) will give the new set of  $z_n$  for the next pulse, to be injected again into (13) and (14) for the next pulse. Cycling through this scheme determines subsequently all future amplitudes.

Appendix D contains output examples of the program of Appendix C. They demonstrate this mechanism with a stable (converging) case and a diverging one, both differing only by a minimally changed parameter. Also some interesting outputs concerning a tune-scan are shown there.

## 3. The Equilibrium Condition

Mathematically there exists an equilibrium state where the system executes exactly repetitive movements from pulse to pulse. For this case all  $N$  cavities – having identical static settings – behave precisely in the same manner. Hence the vector sum feedback forces the same voltage  $V_0$  for all of them and they also feel identically the *nominal* ‘Lorentz kick’  $K_0$  as defined in (10). Therefore

equation (11) is valid for all cavities without distinction and amplitudes exactly repeat under the condition

$$(15) \quad z_{eq} = (z_{eq} - i K_0) \rho \Rightarrow z_{eq} = \frac{-i K_0 \rho}{1 - \rho}$$

The actual frequency deviation from the relaxed state is its real part, thus  $x_{eq} = \text{Re}(z_{eq})$ . The equilibrium constant  $G_{eq}$  from (14) then becomes

$$(16) \quad G_{eq} = V_0 (1 - 2 i x_0); \quad x_0 = x_{tune} + \text{Re}(z_{eq})$$

Intuitively we expect that the system will settle at this equilibrium state after a short transient period. However, as we will prove in the following chapters, this is not always the case.

On closer examination this approach for the equilibrium-state is even somewhat naïve. For stronger detuning there exist in fact other stable equilibrium cases where both cavities do not have equal amplitudes (called ‘split-stable’). Therefore, if an instability starts around the ‘naïve’ equilibrium, it can get caught again in this split state and stay stable there. Also ‘breathing’ can happen when the system walks forward and backward between two nearly stable situations without growing amplitude. One instructive case observed numerically for two cavities is the exchange of equilibrium position from pulse to pulse, thus each cavity comes back to its initial amplitude each second pulse only. All this can be demonstrated straightforwardly with the very small and easily understandable program in Appendix C.

On the other hand if such effects start we are ‘lost’ in any case. Therefore we will not do a (probably very complicated) detailed analysis of these cases. If we can guarantee stability on the ‘naïve’ equilibrium, our RF system will do what it should do. What happens once the instability starts is of a more academic interest.

#### 4. Perturbations around the Equilibrium Condition

Let us assume that the amplitudes  $z_n$  are very close to the (‘naïve’) equilibrium condition and we write with small  $dz_n$  and  $dV_n$

$$(17) \quad z_n = z_{eq} + dz_n$$

$$(18) \quad V_n = V_0 + dV_n$$

We express equation (11) using (17) and (18) and subtract the steady state equation (15) yielding the recursion relation for the deviations

$$(19) \quad dz_{n,new} = \left( dz_{n,old} - i K_0 \left( \left| 1 + dV_{n,old} / V_0 \right|^2 - 1 \right) \right) \rho$$

or to first order

$$(20) \quad dz_{n,new} = \left( dz_{n,old} - i 2 K_0 \text{Re}(dV_{n,old}) / V_0 \right) \rho$$

$V_0$  being a real number. The cavity voltages according to (13) become

$$(21) \quad V_{n,old} = \frac{G}{1 - i 2(x_0 + \text{Re}(dz_{n,old}))}; \quad x_0 = x_{tune} + \text{Re}(z_{eq})$$

or to first order in  $dz_n$

$$(22) \quad V_{n,old} = \frac{G}{1 - 2 i x_0} \left( 1 + \frac{2 i \text{Re}(dz_{n,new})}{1 - 2 i x_0} \right) = G' \left( 1 + \frac{2 i \text{Re}(dz_{n,new})}{1 - 2 i x_0} \right)$$

with a new constant  $G'$ . The normalization condition (14) determines  $G'$  to first order

$$(23) \quad G' = V_0 \left( 1 - \frac{1}{N} \frac{2i}{1-i} \frac{1}{2x_0} \sum_{m=1}^N \operatorname{Re}(dz_{m,old}) \right)$$

thus we get

$$(24) \quad dV_{n,old} = \frac{2i}{1-i} \frac{V_0}{2x_0} \left( \operatorname{Re}(dz_{n,old}) - \frac{1}{N} \sum_{m=1}^N \operatorname{Re}(dz_{m,old}) \right)$$

holding precisely  $\sum_{n=1}^N dV_n = 0$ . The real part of  $dV_n$  is thus to first order

$$(25) \quad \operatorname{Re}(dV_{n,old}) = -\frac{4}{1+4} \frac{V_0}{x_0^2} \left( \operatorname{Re}(dz_{n,old}) - \frac{1}{N} \sum_{m=1}^N \operatorname{Re}(dz_{m,old}) \right)$$

yielding finally the fundamental recursion relation

$$(26) \quad dz_{new,n} = \left( dz_{old,n} + i \xi \left( \operatorname{Re}(dz_{n,old}) - \frac{1}{N} \sum_{m=1}^N \operatorname{Re}(dz_{m,old}) \right) \right) \rho$$

$$(26a) \quad \text{with } \xi = \frac{8}{1+4} \frac{K_0}{x_0^2} = \frac{8}{1+4} \frac{K_0 (x_{tune} + \operatorname{Re}(z_{eq}))}{(x_{tune} + \operatorname{Re}(z_{eq}))^2}$$

## 5. The Equivalent Matrix Equation

In (26) we have to use the real part of  $dz_n$ , thus we split  $dz_n$  into its real and imaginary part,  $dz_n = dx_n + i dy_n$ . We rearrange the  $N$ -fold equations (26) by defining the two  $N$ -vectors  $(dx)$  and  $(dy)$ ,  $(dx)$  having as components  $dx_1$  to  $dx_N$ , and  $(dy)$  the components  $dy_1$  to  $dy_N$ . Furthermore we define the  $2N$ -vector  $((dx),(dy))$  with the components  $(dx_1..dx_N, dy_1..dy_N)$ . The calculations with  $\operatorname{Re}(dz_n)$  can be expressed by a  $N \times N$  matrix  $P$ , having  $-1/N$  in all non-diagonal elements and  $(1-1/N)$  in the diagonal elements

$$(27) \quad P = \begin{pmatrix} 1-1/N & -1/N & \dots & -1/N \\ -1/N & 1-1/N & \dots & -1/N \\ \dots & \dots & \dots & \dots \\ -1/N & -1/N & \dots & 1-1/N \end{pmatrix}$$

yielding

$$(28) \quad \begin{pmatrix} \operatorname{Re}(dz_1) - \frac{1}{N} \sum_{m=1}^N \operatorname{Re}(dz_m) \\ \dots \\ \operatorname{Re}(dz_N) - \frac{1}{N} \sum_{m=1}^N \operatorname{Re}(dz_m) \end{pmatrix} = \begin{pmatrix} dx_1 - \frac{1}{N} \sum_{m=1}^N dx_m \\ \dots \\ dx_N - \frac{1}{N} \sum_{m=1}^N dx_m \end{pmatrix} = P \begin{pmatrix} dx_1 \\ \dots \\ dx_N \end{pmatrix}$$

The multiplication of  $dz_n$  with the complex factor  $\rho$  becomes

$$(29) \quad dz_n \cdot \rho = (\rho_r dx_n - \rho_i dy_n) + i (\rho_i dx_n + \rho_r dy_n)$$



which can also be expressed in matrix form. Then we can write the recursion relation (26) for small amplitudes close to the equilibrium state in matrix form

$$(30) \quad \begin{pmatrix} \{\rho_r - \rho_i \xi P\} & \{-\rho_i\} \\ \{\rho_i + \rho_r \xi P\} & \{+\rho_r\} \end{pmatrix} \begin{pmatrix} dx_{old} \\ dy_{old} \end{pmatrix} = \begin{pmatrix} dx_{new} \\ dy_{new} \end{pmatrix}$$

where all four curly brackets { } correspond to a NxN matrix, the scalars  $\rho_r$ ,  $\rho_i$  and  $\xi$  are to be interpreted as this factor times a NxN identity matrix. To investigate if any initial perturbation grows or decays again, we have to determine all eigenvalues  $\lambda$  of the corresponding eigenvalue equation with the system matrix T

$$(31) \quad T \begin{pmatrix} dx \\ dy \end{pmatrix} = \begin{pmatrix} \{\rho_r - \rho_i \xi P\} & \{-\rho_i\} \\ \{\rho_i + \rho_r \xi P\} & \{+\rho_r\} \end{pmatrix} \begin{pmatrix} dx \\ dy \end{pmatrix} = \lambda \begin{pmatrix} dx \\ dy \end{pmatrix}$$

## 6. Solution of the Eigenvalue Equation

The apparent complexity of the 2Nx2N eigenvalue equation can be reduced due to the fact that only P is a true matrix. All other components are ‘disguised scalars’ – multiplied by an identity matrix – for which any vector is an eigenvector, the eigenvalue being the scalar. Therefore let us assume that we know an eigenvalue  $\mu$  of the matrix P and a corresponding eigenvector  $(dx)_\mu$ .

$$(32) \quad P (dx)_\mu = \mu (dx)_\mu$$

Then the 2N-dimensional equation (31) is equivalent to the two N-dimensional equations

$$(33) \quad (\rho_r - \rho_i \xi \mu - \lambda) (dx)_\mu - \rho_i (dy)_\mu = 0$$

$$(34) \quad (\rho_i + \rho_r \xi \mu) (dx)_\mu + (\rho_r - \lambda) (dy)_\mu = 0$$

These can be solved for a  $(dy)_\mu$  co-linear to  $(dx)_\mu$ , e.g. defined by (33), but also the determinant of the system has to vanish (characteristic polynomial), i.e.

$$(35) \quad (\rho_r - \rho_i \xi \mu - \lambda)(\rho_r - \lambda) + (\rho_i + \rho_r \xi \mu)\rho_i = 0$$

which is solved by

$$(36) \quad \lambda_{\pm} = \rho_r - \frac{1}{2}\xi\mu\rho_i \pm \sqrt{(\rho_r - \frac{1}{2}\xi\mu\rho_i)^2 - |\rho_i|^2}$$

i.e. we obtain two eigenvalues  $\lambda_{\pm}$  for each eigenvalue  $\mu$  of P.

All N eigenvalues  $\mu$  of P can be determined easily. Let us assume a vector  $(dx)_\mu$  where all components are set to ‘1’. Practically this means all cavities have the same amount of voltage dV too much. One sees immediately that P as defined in (27) will transform this vector onto the zero-vector, thus  $\mu=0$ . Practically this means that such a vector cannot survive in the system since there would be a net voltage deviation, in contrast to the system definition that the vector feedback cancels all overall deviations immediately, thus transforming any existing component to zero.

We construct another vector  $(dx)_\mu$  where all components are equal to zero except the first one, set to -1, and a single other component, set to +1. Practically this means that the first cavity has a voltage deviation -dV and the other single cavity the deviation +dV, all others being perfect. Therefore the RF vector sum is correct. This vector will be transformed by P (see (27)) exactly onto itself again, thus  $\mu=1$ . Since we have N-1 possibilities to place the ‘+1’ component, the eigenvalue  $\mu=1$  of P exists N-1 times and any linear combination of these eigenvectors is an eigenvector for this case, all having no total voltage deviation. In practice this means that the feedback does not change any vector that has the design sum voltage. Therefore we have identified all N eigenvalues and eigenvectors of P.

For the unique case  $\mu=0$  the corresponding pair of system eigenvalues  $\lambda_{\pm,0}$  becomes

$$(37) \quad \lambda_{\pm,0} = \rho_r \pm i \rho_i$$

The other pair of eigenvalues  $\lambda_{\pm,1}$  for the case  $\mu=1$  (with multiplicity  $N-1$ ) becomes

$$(38) \quad \lambda_{\pm,1} = \rho_r - \frac{1}{2}\xi\rho_i \pm \sqrt{(\rho_r - \frac{1}{2}\xi\rho_i)^2 - |\rho|^2}$$

Since the  $2N \times 2N$  matrix  $T$  has  $2N$  eigenvalues and we have found one pair and  $(N-1)$  identical pairs, the determined set of eigenvalues is complete.

## 7. Discussion of the Solutions

At each multiplication with the real matrix  $T$  the length of an eigenvector is scaled by the eigenvalue, provided the latter is real. Also for complex eigenvalues a similar statement holds, but the scaling factor is the *absolute* value of the eigenvalue. Some details of this case will be briefly discussed in Appendix B. An initial random perturbation contains contributions from all eigenvectors (see also Appendix B) and for any eigenvalue with absolute value larger than unity, its corresponding eigenvector contribution will not stop to increase, thus the system is unstable. If there are several such eigenvalues, the largest one will dominate the growth. Only if all eigenvalues have absolute values smaller than one, any initial perturbation will decay and the system will settle onto its ‘naïve’ equilibrium state. We will determine now the conditions for which all absolute eigenvalues are smaller than one.

The eigenvalue pair  $\lambda_{\pm,0}$  in (37) is complex and has the absolute value  $|\rho|$ . However,  $\rho$  describes a damped oscillatory movement (see (6)) and therefore its absolute value is always below one. Therefore the eigenvalue pair  $\lambda_{\pm,0}$  cannot cause any instability.

All remaining eigenvalues of  $T$  are  $(N-1)$  identical pairs, thus we have to examine only one pair. For the further discussion of  $\lambda_{\pm}$  in (38) it is convenient to introduce the parameter  $\alpha$

$$(39) \quad \boxed{\alpha = \rho_r - \frac{1}{2}\xi\rho_i \quad \Rightarrow \quad \lambda_{\pm} = \alpha \pm \sqrt{\alpha^2 - |\rho|^2}}$$

For further discussion we consider  $\rho$  as a fixed value, determined by the repetition rate and the cavity mechanical resonance, and vary  $\alpha$  – in fact the parameter  $\xi$  – which is a function of the cavity field and RF tune.

We will have to examine three distinct ranges for  $|\alpha|$

### 7.1 Range 1: $|\alpha| < |\rho|$

The expression under the root in (39) is negative and the *eigenvalues are complex*. We can express (39) then with real and imaginary part as

$$(40) \quad \lambda_{\pm} = \alpha \pm i\sqrt{|\rho|^2 - \alpha^2}$$

with the absolute value squared

$$(41) \quad |\lambda_{\pm}|^2 = \alpha^2 + |\rho|^2 - \alpha^2 = |\rho|^2$$

$\rho$  has an absolute value smaller than one and we conclude

$$(42) \quad |\alpha| < |\rho| \quad \Rightarrow \quad \text{all } |\lambda| = |\rho| < 1 \quad \Rightarrow \quad \text{stability}$$

**7.2 Range 2:**  $|\rho| \leq |\alpha| < \frac{1}{2}(1+|\rho|^2)$

The left inequality guarantees that all eigenvalues are real. The right inequality enforces indirectly  $|\alpha| < 1$  – since  $|\rho|^2$  is smaller than one – and it can be transformed to

$$(43) \quad |\alpha|^2 - |\rho|^2 < 1 - 2|\alpha| + |\alpha|^2 = (1 - |\alpha|)^2$$

In (43) both sides are positive. In this case (43) is equivalent to the same inequality with the *positive* roots. Since  $0 < 1 - |\alpha|$ , we obtain

$$(44a) \quad |\alpha| + \sqrt{|\alpha|^2 - |\rho|^2} < 1$$

Exploiting the fact that  $\alpha > 0 \Rightarrow |\alpha| = \alpha \Rightarrow |\alpha| + \sqrt{|\alpha|^2 - |\rho|^2} = \lambda_+$  we conclude

$$(44b) \quad \text{for } \alpha > 0 \Rightarrow \lambda_+ < 1$$

Multiplying (44a) by  $(-1)$  and inverting the inequality condition yields

$$(44c) \quad -1 < -|\alpha| - \sqrt{|\alpha|^2 - |\rho|^2}$$

Exploiting the fact that  $\alpha < 0 \Rightarrow -|\alpha| = \alpha \Rightarrow -|\alpha| - \sqrt{|\alpha|^2 - |\rho|^2} = \lambda_-$ , we conclude

$$(44d) \quad \text{for } \alpha < 0 \Rightarrow -1 < \lambda_-$$

Trivially the following condition always holds (left we subtract, right we add to  $|\alpha|^2$ )

$$(45) \quad |\alpha|^2 - |\rho|^2 < 1 + 2|\alpha| + |\alpha|^2 = (1 + |\alpha|)^2$$

Both sides are positive, thus (45) is equivalent to

$$(46a) \quad -|\alpha| + \sqrt{|\alpha|^2 - |\rho|^2} < 1 \Rightarrow (\text{for } \alpha < 0 \Rightarrow \lambda_+ < 1)$$

Multiplying (46a) by  $(-1)$  and inverting the inequality condition yields

$$(46b) \quad -1 < |\alpha| - \sqrt{|\alpha|^2 - |\rho|^2} \Rightarrow (\text{for } \alpha > 0 \Rightarrow -1 < \lambda_-)$$

Using the fact that per definition  $\lambda_- \leq \lambda_+$ , we conclude that within ‘range 2’ the inequalities

$$(47) \quad -1 < \lambda_- \leq \lambda_+ < +1$$

always hold, enforced for positive  $\alpha$  by (46b) and (44b), and for negative  $\alpha$  by (44d) and (46a). Therefore, combining ‘range 1’ and ‘range 2’ examined till now, we conclude

$$(48) \quad |\alpha| < \frac{1}{2}(1 + |\rho|^2) \Rightarrow \text{stability}$$

**7.3 Range 3:**  $\frac{1}{2}(1 + |\rho|^2) \leq |\alpha|$

If we assume that  $|\alpha|$  is just on the edge of the above inequality, i.e. as an equality, we have the two cases for positive or negative  $\alpha$

$$(49a) \quad 0 < \alpha = +\frac{1}{2}(1 + |\rho|^2) \Rightarrow \lambda_+ = \alpha + \sqrt{\alpha^2 - |\rho|^2} = +1$$

$$(49b) \quad 0 > \alpha = -\frac{1}{2}(1 + |\rho|^2) \Rightarrow \lambda_- = \alpha - \sqrt{\alpha^2 - |\rho|^2} = -1$$

If for positive  $\alpha$  in (49a) we increase  $\alpha$  by any amount,  $\lambda_+$  increases above +1 and if for negative  $\alpha$  in (49b) we increase its absolute value – i.e. we decrease  $\alpha$  – by any amount,  $\lambda_-$  becomes less than –1. Therefore we conclude:

$$(50) \quad \frac{1}{2}(1+|\rho|^2) < |\alpha| \quad \Rightarrow \quad \textit{instability}$$

The limiting case  $\lambda=\pm 1$ , where an initial perturbation will ring forever with neither growth nor decay, is a mathematical artefact without practical interest. Hence we conclude that (48) covers exclusively *all* stable cases.

#### 7.4 The General Stability Condition

We now re-inject the definition (39) of  $\alpha$

$$(51) \quad |\rho_r - \frac{1}{2}\xi\rho_i| < \frac{1}{2}(1+|\rho|^2) \Leftrightarrow \textit{stability}$$

Going back to the basic definition (6) of  $\rho$  and dividing by  $(|\rho|/2)$  we separate attenuation and phase advance in  $\rho$  and finally obtain the stability condition

$$(52) \quad \boxed{|2 \cos(\psi) - \xi \sin(\psi)| < \left(\frac{1}{|\rho|} + |\rho|\right) \Leftrightarrow \textit{stability}}$$

with

$$(52a) \quad |\rho| = \exp\left(-\pi (f_{mech} / f_{rep}) / Q_{mech}\right); \quad \psi = 2 \pi (f_{mech} / f_{rep})$$

$$(52b) \quad \rho = |\rho| (\cos(\psi) + i \sin(\psi))$$

$$(52c) \quad \xi = \frac{8 K_0 x_0}{1 + 4 x_0^2} = \frac{8 K_0 (x_{tune} + \text{Re}(z_{eq}))}{1 + 4 (x_{tune} + \text{Re}(z_{eq}))^2}$$

$$(52d) \quad K_0 = V_0^2 \omega_{mech} T_1 k_L / (L^2 B) \rightarrow \omega_{mech} k_L / (L^2 B) \int_0^T V^2 dt$$

$$(52e) \quad x_0 = x_{tune} + \text{Re}(z_{eq}); \quad z_{eq} = \frac{-i K_0 \rho}{1 - \rho}; \quad x_{tune} \text{ user tunable}$$

Practically  $\psi$  and  $|\rho|$  are given by the cavity design and linac repetition parameters and these determine the stability limits  $\xi_{low}$  and  $\xi_{up}$  by (52). Therefore we can determine for an assumed field level and RF pulse length the parameter  $K_0$ . This determines the limits  $\eta_{up} = \xi_{up} / (2K_0)$  and  $\eta_{low} = \xi_{low} / (2K_0)$  of the function  $\eta = (4 x_0) / (1 + 4 x_0^2)$ ;  $\eta$  is bound by the absolute value 1. Then all cases with a tune status  $x_0$  – which is the cavity detuning (in bandwidths) at the instant ‘RF on’ is required – within this range are stable. We have depicted this function with hypothetical limits – the general case – in fig. 3. We find a central stable region enclosed by two unstable regions. Outside we have again two stable regions but they are of no practical interest since the cavities are far out of tune and the RF power would be excessive. If  $\eta_{up}$  would be larger than 1, the upper unstable region would vanish; if also  $\eta_{low}$  would be smaller than –1, all unstable regions would disappear. This is only possible for very low  $K_0$ , equivalent to very low field

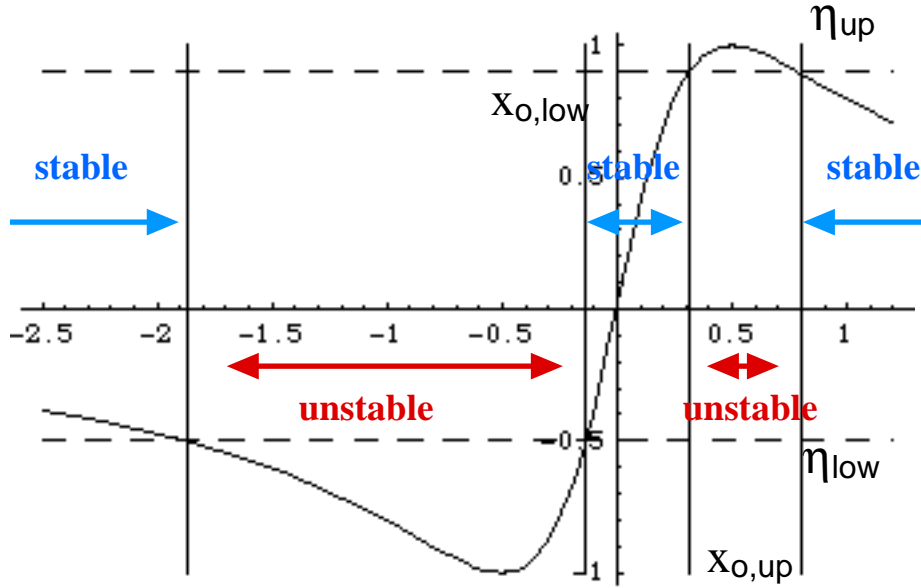


Fig 3: Stable and unstable regions. Dashed lines are the limits  $\eta_{up} = \xi_{up}/(2K_0)$  and  $\eta_{low} = \xi_{low}/(2K_0)$ , the corresponding ‘inner limits’  $x_{up}$  and  $x_{low}$  are depicted as vertical lines as well as the ‘outer limits’. Whenever  $\eta = \xi/(2K_0)$  is between the limits  $\eta_{up}$  and  $\eta_{low}$ , the system is stable. If  $|\eta|>1$ , the corresponding instability region disappears and if both  $|\eta_{low}|>1$  and  $|\eta_{up}|>1$  the system is stable for all tuner positions.

## 8. GENERAL PRACTICAL IMPLICATIONS

### 8.1 Cavity mechanically ‘on tune’ or ‘anti-tune’

The right-hand side of (52) is always larger than two for  $|\rho|<1$ . Therefore we see that for  $\sin(\psi)=0$ , the system is always stable. There are two possibilities to realise this condition.

One is a cavity ‘mechanically on tune’, i.e. it makes an integer number of oscillations within the linac repetition time. Then stability exists despite the fact that the mechanical oscillation of the cavity may become huge due to this resonant condition. This strong excitation will probably cause material fatigue and will be avoided by the mechanical engineers. Also the cavity RF frequency will change considerably during the – in reality not infinitely short – ‘RF on time’ when the mechanical amplitude is high.

The second possibility is a cavity ‘mechanically on anti-tune’, i.e. it executes exactly a half-integer number of oscillations within the linac repetition. This condition coincides also with the smallest mechanical amplitude and is therefore very attractive. However, it is very difficult to hit exactly this condition. Therefore we should assume  $\sin(\psi)\neq 0$  for a realistic design, and maybe also exclude  $\sin(\psi)$  being *very* small.

### 8.2 Is there an intrinsically stable set-up ?

For  $\sin(\psi)\neq 0$ , by increasing  $\xi$ , it is always possible – at least on paper – to break the condition (52), thus there is no realistic set-up that is intrinsically free from instabilities up to all field levels.

### 8.3 Is there a preferred mechanical cavity frequency condition ?

If we would change the cavity design such that the angle  $\psi$  goes to  $\psi'=\psi+\pi$ , i.e.  $\sin(\psi')=-\sin(\psi)$  and  $\cos(\psi')=-\cos(\psi)$ , the condition (52) is broken at exactly the same  $\xi$  since the absolute value enters on the left-hand side.

If we would change the cavity design such that the angle  $\psi$  goes to  $\psi'=\psi+\pi/2$ , i.e. either  $\sin(\psi')$  or  $\cos(\psi')$  change their sign and the other one not, the condition (52) is broken at exactly the same absolute  $|\xi|$  but with opposite sign.

Therefore there is no preferential ‘quadrant’, only the total distance from the closest mechanical resonance condition is important.

#### 8.4 Can we guarantee $\xi=0$ ?

If we could guarantee always that  $\xi=0$  (very small), there would also be no instability, independent of the cavity mechanical conditions. We can assume that the cavity is already designed with a minimum possible Lorentz constant  $k_L$  and the design voltage is an external constraint, thus we have no handle on  $K_0$  any more (see (52c)). The other parameter is  $x_0$ , representing the cavity tune status at the instant when ‘RF on’ is required. It can in theory always be tuned to zero since it is a sum (see (52e)) where one term is the RF tune-setting  $x_{\text{tune}}$  of the cavity. However there is one technical difficulty. If we change the design voltage,  $K_0$  and with it the equilibrium position  $z_{\text{eq}}$ ,  $x_{\text{eq}}=\text{Re}(z_{\text{eq}})$  changes. Therefore each voluntary or involuntary change of the operational voltage of the cavity has to be followed by a corresponding change of tuner setting (which is also in the interest of minimising the necessary RF power). An additional difficulty arises due to the fact that in a real machine there is not an exact instant of ‘RF on’ as used for our model. In reality there is a certain lap of time while RF is on during which the cavity RF frequency changes. Therefore  $x_0$  becomes more difficult to measure to drive a tuner feedback to keep  $\xi$  small.

The condition (52) gives the allowable range within which  $x_0$  has to be kept to avoid this instability.

$\xi$  also becomes small if  $x_0$  gets very large. However, this idea is not realistic since this means to work with a strongly detuned cavity requiring forbidding RF power.

#### 8.5 Is there a most safe tuner position ?

There are two ways to break (52), a positive and a negative one. For the discussion we assume that the mechanical frequency is in the quadrant with  $\cos(\psi)>0$  and  $\sin(\psi)>0$ ; other quadrants are identical except the choice of signs (see 8.3). The two limit conditions become then with  $L = (|\rho|+1/|\rho|)$

$$(53) \quad 2 \cos(\psi) - \xi_{\pm} \sin(\psi) = \pm L \Rightarrow \xi_{\pm} = \frac{2 \cos(\psi) \pm L}{\sin(\psi)}$$

The ‘central point’ of both limits is their average

$$(54) \quad \xi_{\text{cent}} = \frac{2 \cos(\psi)}{\sin(\psi)} = 2 \cot(\psi)$$

and the ‘problem free’ range has the width

$$(55) \quad \Delta\xi = \pm \frac{L}{\sin(\psi)} \approx \pm \frac{2}{\sin(\psi)}$$

where we have approximated  $L$  by 2 (valid for a not too strong attenuation). However, this consideration is not always applicable since a voluntary static detuning by  $\xi$  (see e.g. (13)) means an overpower of

$$(56) \quad \frac{P_{RF}}{P_{RF,\min}} = \frac{1 + 4 \xi_{\text{cent}}^2}{1}$$

prohibitive for larger  $\xi$ .

## 9. NUMERICAL EXAMPLES

First, we derive an approximation formula. In reality the cavities will be loaded and unloaded in a finite time and have a beam pulse of finite length. We assume that loading has about a linear rise, the beam pulse the field is constant and unloading takes place with the system energy decay time constant  $\tau_U = Q_{ext} / \omega_{RF}$ . Therefore we have to replace  $T_1$  in (52d) by

$$(57) \quad \langle T_1 \rangle \rightarrow \frac{1}{V_0^2} \int_0^T V^2(t) dt = \left( \frac{1}{3} T_{rise} + T_{beam} + \frac{Q_{ext}}{\omega_{RF}} \right)$$

For the following analysis we use the stability criterion given in (52).

### 9.1 SPL

For SPL [2] it was planned to run with 75 Hz repetition rate<sup>1</sup> and the LEP2 cavities – probably similar to the planned  $\beta=0.8$  cavities – have the main resonance very close to 100 Hz. As mechanical Q-value we have assumed 38 (in the ballpark between 20 and 50 matching the LEP2 cavity observations), so we have

$$(58) \quad \cos(\psi) = -0.5; \quad \sin(\psi) = 0.866; \quad |\rho| = 0.896 \rightarrow |\rho| + \frac{1}{|\rho|} = 2.012$$

The stability condition (52) then becomes  $|\xi - 0.866 + 1| < 2.012$ , i.e. we remain stable for  $\xi_{low} = -3.478 < \xi < +1.169 = \xi_{up}$ .

The SPL RF frequency is 352 MHz with a  $Q_{ext}$  of  $3 \cdot 10^6$ , thus  $B=117$  Hz. The Lorentz constant was measured to  $-2$  Hz/(MV/m)<sup>2</sup>, the rise time is  $T_{rise}=2$  ms, and the beam pulse  $T_{beam}=2.2$  ms, thus we get with the formula (57)  $\langle T_1 \rangle = 4.2$  ms yielding

$$(59) \quad K_0 = V_0^2 \omega \langle T_1 \rangle k_L / (L^2 B) = E_{acc,0}^2 \omega \langle T_1 \rangle k_L / B = -4.5 \cdot 10^{-2} \cdot E^2 [MV/m]$$

Using the definition (52c) for  $\xi$  and the abbreviation  $\eta = 4 x_0 / (1 + 4x_0^2)$  – i.e. we have  $\xi = 2 \eta K_0$  – we keep stability for

$$(60) \quad -12.99 / E^2 [MV/m] < \eta < 38.64 / E^2 [MV/m]$$

From the definition  $\eta = 4 x_0 / (1 + 4x_0^2)$  we see (fig. 3) that its absolute maximum is 1. Therefore as long as E is below  $\sqrt{12.99}$  MV/m = 3.6 MV/m, we are safe for *all* tuner settings. If we stay below  $\sqrt{38.64}$  MV/m = 6.2 MV/m, there is an infinitely large stable range for positive detuning but an unstable region for negative detuning. From  $\eta$  we get  $x_0$  by

$$(61) \quad x_0 = \frac{1}{2\eta} \left( 1 \pm \sqrt{1 - \eta^2} \right)$$

where we have to take the negative root for the limit closer to the central region. Let us assume now that we try to run at 2, 6, 8, 9, 10 and 11 MV/m. We get the following table:

<sup>1</sup> Updated plans talk of 50 Hz, thus the main cavity frequency becomes be a multiple of the repetition frequency ....

E [MV/m]	K0	$\eta$ .low	$\eta$ .up	x0.low	x0.up	x0'.low	x0'.up	$\Delta f$ [Hz]
2	0.18	-9.6611	3.2472	$\infty$	$\infty$	$\infty$	$\infty$	$\infty$
6	1.62	-1.0735	0.3608	$\infty$	0.0933	$\infty$	2.6783	$\infty$
8	2.88	-0.6038	0.2030	-0.1680	0.0513	-1.4881	4.8760	25.65
9	3.645	-0.4771	0.1604	-0.1270	0.0404	-1.9691	6.1957	19.58
10	4.5	-0.3864	0.1299	-0.1005	0.0326	-2.4872	7.6663	15.58
11	5.445	-0.3194	0.1073	-0.0820	0.0269	-3.0491	9.2887	12.74

Table 1: Stable limits for 2, 6, 8, 9, 10 and 11 MV/m cavity operation in SPL as predicted by the model calculations.  $\Delta f$  is the range between  $x_{0,low}$  and  $x_{0,up}$  transformed into Hz

For comparison we have done simulations with ‘SPLinac’ with two cavities connected to one transmitter, we have allowed a limit 2 MW of RF power, largely overpowered to be as independent as possible of small changes during cavity loading.

For a chosen field level we have scanned the static detuning; the absolute setting is less important since it is difficult to define the cavity frequency swing  $x_{eq} = \text{Re}(z_{eq})$  at the ‘instant’ of ‘RF on’ since in reality this is a lap of time during which the frequency moves. First we have searched for a field level at which there is no instability for any tune setting; predicted were 3.6 MV/m. However, we found instabilities at negative tune settings for fields as low as 2.5 MV/m, but none at 2 MV/m. Table 2 shows the results.

$\Delta f / f_0$ [ $10^{-7}$ ]	$\Delta f$ [Hz]	observation
<b>-6</b>	<b>-211.2</b>	<b>stable</b>
<b>-4</b>	<b>-140.8</b>	<b>stable</b>
<b>-2</b>	<b>-70.4</b>	<b>stable</b>
<b>-1</b>	<b>-35.2</b>	<b>stable</b>
<b>0</b>	<b>0</b>	<b>stable</b>
<b>1</b>	<b>35.2</b>	<b>stable</b>
<b>2</b>	<b>70.4</b>	<b>stable</b>

Table 2: Simulation with ‘SPLinac’ for the same case with E=2 MV/m, cavity frequency swing  $-13$  to  $+8$  Hz, centre at  $-2.5$  Hz

The model predicts that there is an infinitely large stable range for positive detuning but instability for negative detuning if we stay below 6.17 MV/m. In the simulation we have tested the field level of 6 MV/m, table 3 shows the results, they behave as predicted by the model.

$\Delta f / f_0$ [ $10^{-7}$ ]	$\Delta f$ [Hz]	observation
0	0	unstable
1	35.2	unstable
2	70.4	unstable
3	105.6	unstable
<b>3.1</b>	<b>109.12</b>	<b>stable</b>
<b>4</b>	<b>140.8</b>	<b>stable</b>
<b>5</b>	<b>176</b>	<b>stable</b>
<b>6</b>	<b>211.2</b>	<b>stable</b>
<b>7</b>	<b>246.4</b>	<b>stable</b>
<b>8</b>	<b>281.6</b>	<b>stable</b>
<b>9</b>	<b>316.8</b>	<b>stable</b>
<b>10</b>	<b>352</b>	<b>stable</b>
<b>12</b>	<b>422.4</b>	<b>stable</b>

Table 3: Simulation with ‘SPLinac’ for the same case with E=6 MV/m, cavity frequency swing  $-120$  to  $+79$  Hz, centre at  $-20.5$  Hz



Therefore we have simulated a field level of 8 MV/m and in fact, as predicted by the model, there is instability below *and* above a small stable range. Table 4 shows the corresponding results.

Two new effects appeared here, one called ‘split-stable’. When pulsing, both cavities behave completely identically for quite a few pulses but then start to separate as in the standard unstable cases. However, after a few pulses the assumed growth stops and a new equilibrium is established with the two cavities slightly distinct, but the pattern exactly repeating from pulse to pulse. Similar behaviour can be found with the simple model simulation program of Appendix C. The second effect was called ‘breathing’. It starts as all instabilities do but stops growing and settles on a pattern that does not repeat from pulse to pulse but that executes limited changes. This can be attributed to non-linearities in the system.

$\Delta f / f_0 [10^{-7}]$	$\Delta f$ [Hz]	observation
3	105.6	unstable
4	140.8	unstable
5	176	unstable
5.7	200.64	unstable
<b>5.8</b>	<b>204.16</b>	<b>stable</b>
<b>6</b>	<b>211.2</b>	<b>stable</b>
<b>7</b>	<b>246.4</b>	<b>stable</b>
<b>7.7</b>	<b>271.04</b>	<b>stable</b>
7.8	274.56	split-stable
8	281.6	split-stable
8.1	285.12	breathing
8.3	292.16	breathing
8.4	295.68	unstable
10	352	unstable
12	422.4	unstable

Table 4: Simulation with ‘SPLinac’ for the same case with E=8 MV/m cavity frequency swing  $-217$  to  $+142$  Hz, centre at  $-37.5$  Hz; stable range 67 Hz

Finally we have increased the field to 10 MV/m and there is no principal change compared to the 8 MV/m case but the stable range is smaller. Table 5 shows the results.

$\Delta f / f_0 [10^{-7}]$	$\Delta f$ [Hz]	observation
8.7	306.24	unstable
<b>8.8</b>	<b>309.76</b>	<b>stable</b>
<b>9</b>	<b>316.8</b>	<b>stable</b>
<b>9.2</b>	<b>323.84</b>	<b>stable</b>
<b>9.4</b>	<b>330.88</b>	<b>stable</b>
<b>9.6</b>	<b>337.92</b>	<b>stable</b>
9.8	344.96	split-stable
10	352	breathing
10.3	362.56	breathing
10.2	359.04	breathing
10.4	366.08	unstable

Table 5: Simulation with ‘SPLinac’ for the same case with E=10 MV/m, cavity frequency swing  $-328$  to  $+220$  Hz, centre at  $-54$  Hz; stable range 28 Hz

We have seen that the model predicts quite well the simulated behaviour, only the precise field levels at which a transition occurs and how wide the stable range is, differ by a factor 2-3 in range, but much less for the threshold fields. However, this can partly be explained by the non-linearities that shift the equilibrium status differently from the predicted by the linear model.

We have also simulated with ‘SPLinac’ cases at 10 MV/m at the edge of instability. The system was set up with 2, 4, 8 or 16 cavities connected to a single transmitter without any other change of parameter, except the transmitter power limit scaled with the number of cavities. For all set-ups at the start the system settled on an equilibrium, seemed to stay on it, but after more than 100 pulses the instability that was hidden before reached visible size and drove the system into a chaotic movement. This demonstrates well the independence of the instability condition from the number of connected cavities.

## 9.2 TESLA

TESLA [3] runs at 5 Hz repetition rate; the main mechanical resonance [4] has a frequency around 280 Hz and a Q-value of about 20, thus  $|\rho|=1.5 \cdot 10^{-4}$ . This attenuation is so strong – the repetition frequency being much lower than the mechanical frequency – that there is so to say no coupling from pulse to pulse. Therefore the limiting value ( $|\rho|+1/|\rho|$ ) of (52) is so large, that any reasonable  $\xi$  is allowed without risking a control instability. This fact is certainly welcome to the TESLA team. On the other hand if *for a test* the TESLA cavities cannot be pulsed much faster than 5 Hz (even the foreseen option of 10 Hz is largely insufficient) the threshold cannot be approached and no useful experimental comparisons can be made with these calculations.

## 10. CONCLUSIONS

We have shown in this paper that there can be a real problem in a pulsed RF system when a single transmitter supplies *several* cavities that feel sensitive Lorentz detuning. The model used is based only on simple assumptions and basic physics laws but still very close to the real object.

We have found with the model that

- For very low field there is no instability at all, independent of the tuner setting
- For medium field level instability appears on one side of the tuning range, the other side remains stable. Which side this is depends on the ratio of cavity mechanical resonance and the machine repetition frequency
- For high field level – and this is the range of planned operational fields – a central stable tuning region is enclosed by instability regions on both sides. This is in contrast to the classical ponderomotive instability which ‘works’ only on one side of the tune range<sup>2</sup>. The width of this central stable region shrinks with rising operational field and can become rather small causing operational difficulties. Further outside are stable regions again but these are of no practical interest (very large detuning requiring large RF overpower).
- The threshold is independent of the number of cavities connected to the unique transmitter (provided there are at least two).

The same principal findings were made with simulations of the same RF systems with ‘SPLinac’, which models all details of cavity loading, unloading and RF power limit with vector sum feedback (all ‘real-world errors’ were set to zero). Evidently the numerical thresholds differ somewhat between the model calculations and the more detailed simulations. However, in view of the concordant findings, one can have confidence that ‘SPLinac’ describes such a system correctly. Hence, any problem encountered there has to be taken seriously.

To circumvent the general problem of this control instability, it might be envisaged to use a more intelligent ‘detector’ than a straight vector sum. However, as intelligent as the controller might be, with only one handle – the RF power – nothing more can be done with this additional knowledge. The only way out is supplying additional handles, either a single transmitter per cavity, a rapid tuning system much faster than the cavity oscillation period or a fast mechanical actuator [5] controlling the individual cavity movements (which then also partly acts as fast tuner).

---

<sup>2</sup> There are several analysis of ponderomotive oscillations; the author has done one for LEP2, including growth rate plots positive on one, negative on the other tune side (CERN-SL Note 95-119 (RF) (1995))

## APPENDIX A: EXAMPLE FROM 'SPLINAC'

The example shows a RF system with two cavities starting up at 10 MV/m. The **sum voltage (zero suppressed) is drawn in blue, quadrature sum voltage in green, both cavity movement/detuning in black** (these traces of both cavities graphically overlap at the beginning). The system seems to settle on a repetitive equilibrium but after about 75 pulses the instability that is hidden till then has grown to visible size, completely taking over soon after.

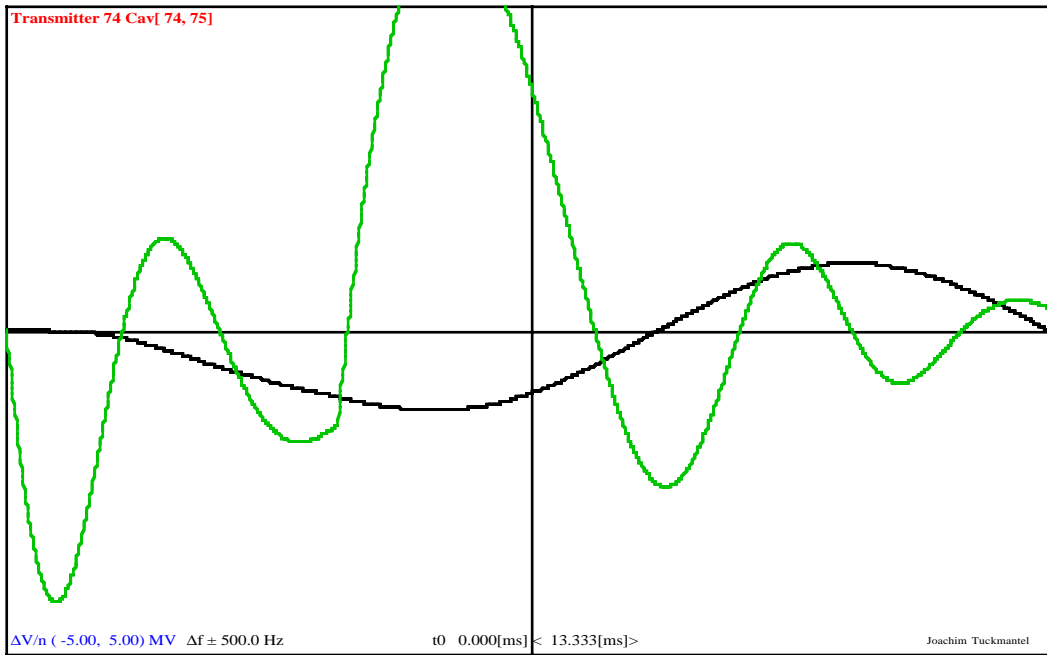


Fig A1: Start at pulse 1 with cavities at rest

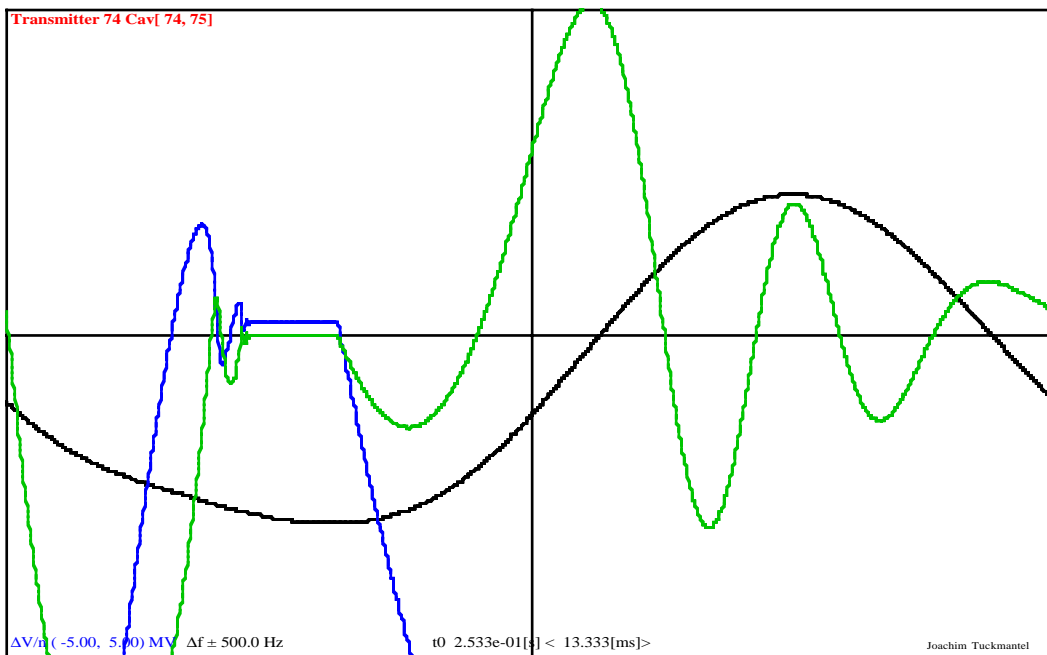


Fig A2: Equilibrium stabilized at about pulse 20

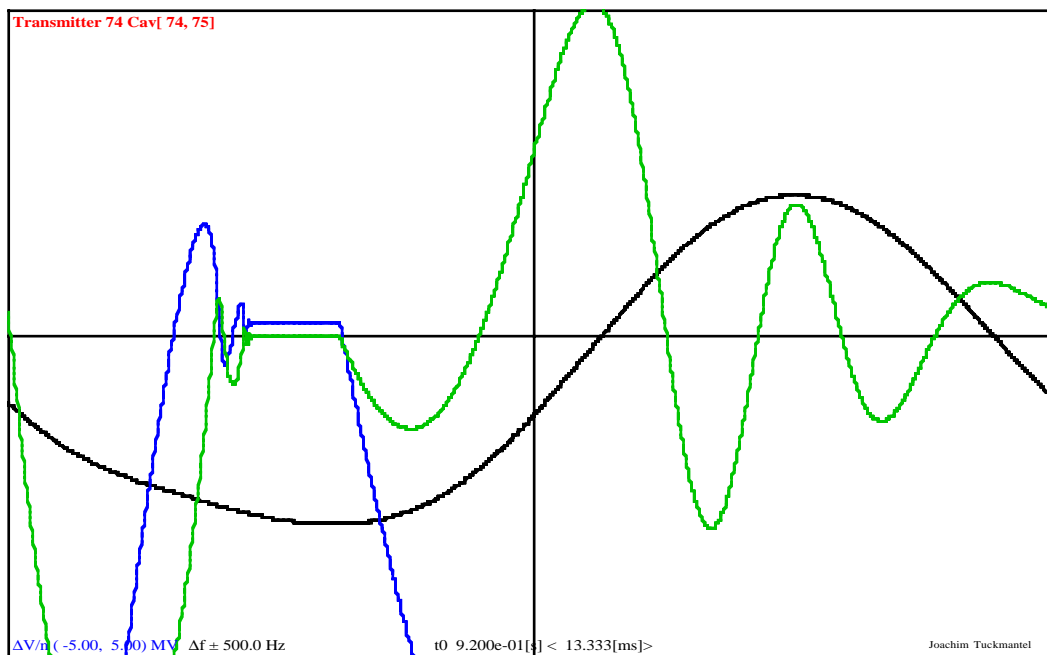


Fig A3: Still running on equilibrium at pulse 70, at least it looks like ....

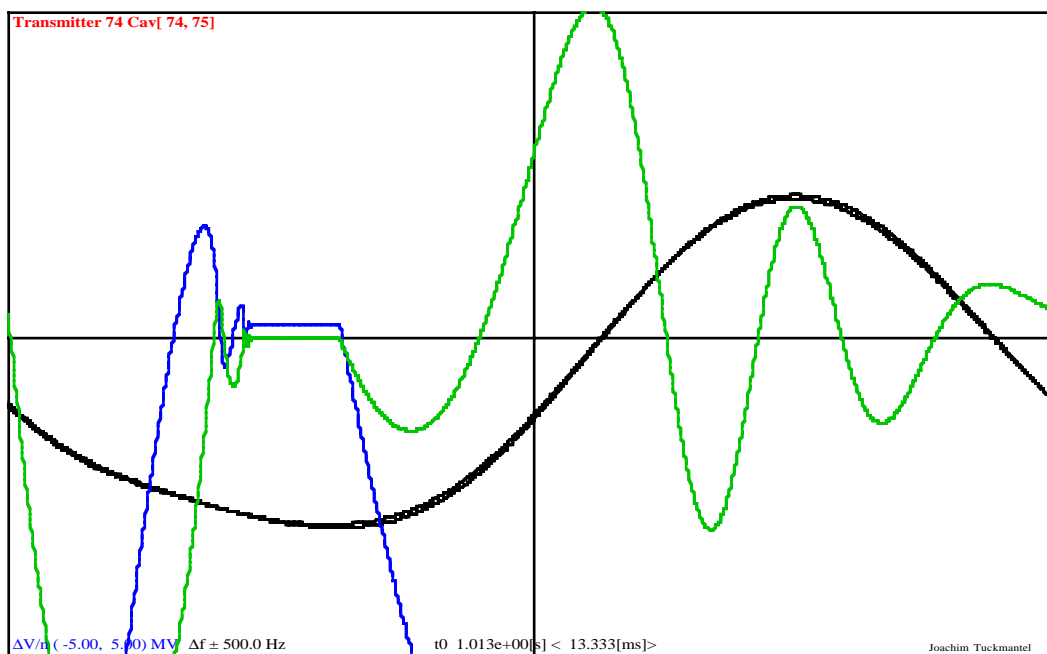


Fig A4: First indication of separation of the two cavity movements at pulse 77

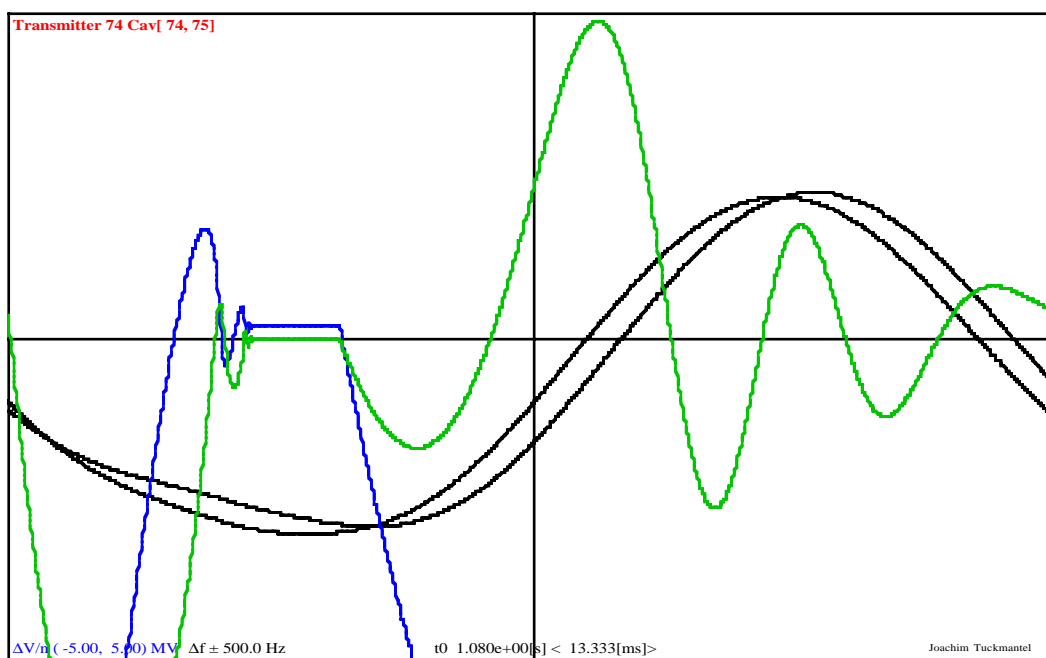


Fig A5: Clear separation of the two cavity movements at pulse 82

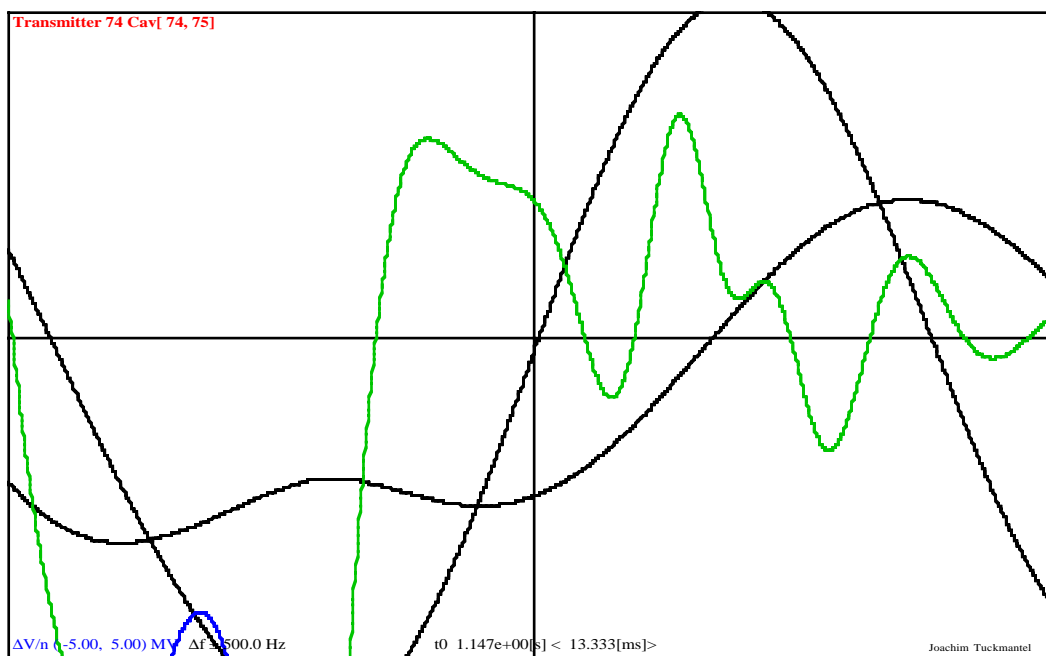


Fig A6: Irrecoverable chaotic movement after pulse 87

## APPENDIX B: COMPLEX EIGENVALUES FOR REAL MATRICES

We will open a parenthesis here concerning the question of complex eigenvalues of a real matrix  $T$  in an  $N$ -dimensional real vector space – thus with real vectors exclusively – which at first looks contradictory. When the characteristic polynomial of  $T$  contains a ( $2^{\text{nd}}$  order) factor irreducible with real roots, we consider  $T$  as a complex matrix that has ‘accidentally’ a zero imaginary part. Then we obtain a complex conjugate eigenvalue pair. In this case there exist no real eigenvectors but a 2-dimensional real eigenspace – a plane embedded in the  $N$ -dimensional vector space – spanned by two real vectors<sup>3</sup>.  $T$  images any vector in this plane onto another vector in this plane and ‘in average’ scaled in length by the **absolute value** of the **complex** eigenvalue.

To demonstrate above statements, let us assume that the *real* Matrix  $T$  has a (unique) complex eigenvalue  $\lambda=a+i*b$ , with *real*  $a$  and  $b$ , and the corresponding complex eigenvector  $A+ i*B$ ,  $A$  and  $B$  having  $N$  *real* components each, thus

$$(B1) \quad T (A + iB) = (a + ib) (A + iB) = (aA - bB) + i (aB + bA)$$

Since  $T$  is real, it is identical to its conjugate. Therefore we get immediately the other eigenvalue and the corresponding eigenvector in conjugating (B1)

$$(B2) \quad T (A - iB) = (a - ib) (A - iB) = (aA - bB) - i (aB + bA)$$

Adding or subtracting (B1) and (B2) yields the *purely real* equations

$$(B3) \quad T A = a A - b B$$

$$(B4) \quad T B = b A + a B$$

and in the following demonstration we will not use complex numbers any more. We can define now a  $2N \times 2N$  equation expressing  $T^m A$  and  $T^m B$ . In fact, the above equations (B3) and (B4) can be combined as

$$(B5) \quad \begin{pmatrix} T & 0 \\ 0 & T \end{pmatrix} \begin{pmatrix} A \\ B \end{pmatrix} = \begin{pmatrix} a I & -b I \\ b I & a I \end{pmatrix} \begin{pmatrix} A \\ B \end{pmatrix}$$

where ‘0’ is a  $N \times N$  zero-matrix and  $I$  the  $N$ -dimensional identity matrix. The matrix on the right hand side can in fact be interpreted as a 2-dimensional rotation matrix multiplied with a scaling factor, the latter is the absolute value of  $|\lambda| = \sqrt{a^2 + b^2}$ . Therefore we can rewrite (B5) as

$$(B6) \quad \begin{pmatrix} T & 0 \\ 0 & T \end{pmatrix} \begin{pmatrix} A \\ B \end{pmatrix} = |\lambda| \begin{pmatrix} \cos(\psi) I & -\sin(\psi) I \\ \sin(\psi) I & \cos(\psi) I \end{pmatrix} \begin{pmatrix} A \\ B \end{pmatrix}$$

with  $\tan(\psi) = b/a$  and  $|\lambda| = \sqrt{a^2 + b^2}$ . A product of two (2-dimensional) rotation matrices is a rotation matrix itself with an angle corresponding to the sum of the two angles. Therefore we can write immediately

$$(B7) \quad \begin{pmatrix} T^m & 0 \\ 0 & T^m \end{pmatrix} \begin{pmatrix} A \\ B \end{pmatrix} = |\lambda|^m \begin{pmatrix} \cos(m\psi) I & -\sin(m\psi) I \\ \sin(m\psi) I & \cos(m\psi) I \end{pmatrix} \begin{pmatrix} A \\ B \end{pmatrix}$$

---

<sup>3</sup> If the same eigenvalue exists  $M$  times, there is an eigenspace of  $2M$  vectors. In fact this situation is even the case here since  $T$  has  $N-1$  identical eigenvalue pairs. But the important fact is (for more details for the case  $M>1$  see any textbook on linear algebra) that – exactly as for  $M=1$  demonstrated here - each vector of this  $2M$  dimensional eigenspace is imaged onto another vector in this eigenspace and the *change in vector-length* is *always* governed by the *absolute value of the eigenvalue*.

Any initial vector  $\alpha A + \beta B$  from this eigenspace, is imaged by  $T^m$  then as

$$(B8) \quad T^m(\alpha A + \beta B) = |\lambda|^m \left( (\alpha A + \beta B) \cos(m\psi) + (\beta A - \alpha B) \sin(m\psi) \right)$$

Having two not necessary orthogonal vectors C and D, we can try the ‘Ansatz’

$$(B9) \quad C \cos(\psi) + D \sin(\psi) = E \cos(\psi + \gamma) + F \sin(\psi + \gamma)$$

with *orthogonal* vectors E and F, i.e.  $E \bullet F = 0$  and the still free parameter  $\gamma$ . With some algebra it can be shown that choosing

$$(B10a) \quad \gamma = \frac{1}{2} \arctan\left(\frac{2 C \bullet D}{D \bullet D - C \bullet C}\right) \quad \text{and}$$

$$(B10b) \quad \begin{aligned} E &= +D \sin(\gamma) - C \cos(\gamma) \\ F &= -D \cos(\gamma) - C \sin(\gamma) \end{aligned}$$

we can fulfil (B9) for all  $\psi$  with orthogonal vectors E and F. Therefore, choosing

$$(B11) \quad C = \alpha A + \beta B; \quad D = \beta A - \alpha B$$

we get E and F according (B10) and obtain finally for *orthogonal* E and F

$$(B12) \quad T^m(\alpha A + \beta B) = |\lambda|^m (E \cos(m\psi + \gamma) + F \sin(m\psi + \gamma))$$

With rising m the image vector is ‘walking’ on the border of an ellipse scaled in size by the factor  $|\lambda|^m$  – ‘modulated’ in length by the ratio of the half-axis E and F. Using the orthogonality of E and F, we can express the absolute square of the vector (B12) as scalar product with itself

$$(B13) \quad \|T^m(\alpha A + \beta B)\|^2 = |\lambda|^{2m} (\|E\|^2 \cos^2(m\psi + \gamma) + \|F\|^2 \sin^2(m\psi + \gamma))$$

Assuming  $\|E\| \geq \|F\|$ , we can get from (B13) the two inequalities<sup>4</sup>

$$(B14) \quad |\lambda|^m \|E\| \geq \|T^m(\alpha A + \beta B)\| \geq |\lambda|^m \|F\|$$

Therefore, the length of the m<sup>th</sup> vector has a lower and an upper bound proportional to  $|\lambda|^m$ . Provided  $F \neq 0$  we have shown that if  $|\lambda| > 1$ , there is an unlimited growth, if  $|\lambda| < 1$  the vector length will be forced towards zero, both governed by the factor  $|\lambda|^m$ .

In the special case  $F=0$  we have  $E \neq 0$  (else both eigenvectors A and B would be zero-vectors), hence the upper bound remains valid, i.e. for  $|\lambda| < 1$  the vector length tends to zero. For the lower bound we express (B13) with  $F=0$

$$(B15) \quad \|T^m(\alpha A + \beta B)\| = |\lambda|^m \|E\| |\cos(m\psi + \gamma)|$$

In fact the vector (B15) may even become zero ‘from time to time’, but since  $E \neq 0$  for  $F=0$ , there is – mathematically speaking – no finite upper bound larger than all vectors (B15) for any m, hence also for  $F=0$  unlimited growth is guaranteed for  $|\lambda| > 1$ .

Therefore clearly a complex eigenvalue with absolute value larger than one corresponds to unlimited growth (till non-linearities take over), for an absolute value smaller than one the corresponding eigenvalue component(s) will tend to zero. That the same statement also holds if the eigenvalue is purely real seems evident.

Finally, if the system has many different eigenvalues, a single one with an absolute value larger than one is sufficient to drive an instability, even if the transients corresponding to all the other

---

<sup>4</sup> the case  $\|F\| \geq \|E\|$  can be demonstrated similarly

eigenvalues decay. Only if *all* absolute values are smaller than one, *all* transients will decay and the system will settle on its equilibrium state.



## APPENDIX C: SHORT PROGRAM LISTING ‘PULSE-TO-PULSE’

Following is the listing of an easy to understand program demonstrating the sudden transition from stability to instability, in comparing runs with the field  $E_0$  different by 0.1%. The program was written in *simple* ‘self-explaining’ standard ANSI C; hence a version in the reader’s favorite language should be straightforward. Since complex variables do not exist in ANSI C, complex multiplication and division are expressed by real variables, making the core code longer than might be possible. In fact, a C++ version with a ‘complex’ class is considerably shorter<sup>5</sup>. Two compressed outputs have been added (Appendix D), one stable with  $E_0=10$  MV/m and one unstable with  $E_0=10.01$  MV/m, else unchanged parameters, as well as a tune-scan.

Another study worthwhile (see Appendix D) is keeping  $E_0=10$  MV/m fixed (constant operational voltage) but ‘play with the tuner’ in changing the cavity RF tune expressed in bandwidths, called ‘xtune’. The system at far out negative tune  $xtune=-6.38$  is at the limit stable (eigenvalue  $-0.9964$ ). Increasing the tune at e.g.  $xtune=-5$ , shows instability but the system soon settles on a new (‘non-naïve’) equilibrium where both cavities exchange their amplitude, coming back after two pulses only(‘breathing’). Increasing the tune further – including crossing the cavity resonance at  $xtune=0$  – stays in the unstable range till  $xtune=1.2610$  (eigenvalue  $-1.0241$ ) and entering the stable region at  $xtune=1.26120$  (real eigenvalue  $-0.9985$ ). In about the center of the stable region at  $xtune=1.3$  we have complex eigenvalues  $(-0.3612 \pm i*0.8196)$  having an absolute value equal to  $|\rho|$ . We are still stable at  $xtune=1.3942$  (real eigenvalue  $0.985$ ) but become unstable again at  $xtune=1.3944$  (eigenvalue  $1.0105$ ). At  $xtune=1.4$  we are unstable but the system settles on another ‘non-naïve’ equilibrium where each cavity has a repetitive position, but not identical for both cavities(‘split-stable’). At  $xtune=3.780$  we are still unstable (eigenvalue  $1.0043$ ) but enter the far out positive stable range at  $xtune=3.783$  (eigenvalue  $1.0043$ ). This behavior resembles very much to the simulations done with ‘SPLinac’.

Have fun in playing with the parameters ...

```
#include <stdio.h>
#include <math.h>
void DoOnePulse( void );
void SetEquil( void );
void Eigenvalues( );
/* global variables accessible from all functions */
double E0,V1Re,V1Im,V2Re,V2Im,z1Re,z1Im,z2Re,z2Im,kick1,kick2;
double Pi,xtune,kick0,rhoRe,rhoIm,rhoAbs,rhoPhi;

int main(void)
{
    int i;
    Pi = 3.1415926536;
    /***** set up system constants *****/
    rhoAbs = exp(-Pi*(100./75.)/38.); /* attenuation in T */
    rhoPhi = (100./75.)*(2.*Pi); /* phase adv. in T (radian)*/
    xtune = 1.2612; /* static detuning in BW */
    /* ---- here chose: stable or unstable ----- */
    E0 = 10.; /* field in MV/m */
    /*E0 = E0 + 0.01; /* drives it unstable */
    kick0 = -4.5E-2*E0*E0; /* SPL Lorentz kick */
    /******/
    rhoRe = rhoAbs*cos(rhoPhi);
    rhoIm = rhoAbs*sin(rhoPhi);
    printf(" |rho| %12.5e phiDeg %7.3f xtune %10.5f E0 %8.5f\n",
           rhoAbs,rhoPhi*180./Pi,xtune,E0);
    /* ---- here chose: starting condition ----- */
    z1Re = 0.; /* zero start condition ... */
    z1Im = 0.;
    z2Re = 0.;
    z2Im = 0.;
```

<sup>5</sup> Not considering the class library, evidently ...

```

SetEquil( );          /* or <<OPTIONAL>> equilibrium start .. */
Eigenvalues( );      /* calculate eigenvalues <<OPTIONAL>> */
z1Re = z1Re + 1.E-8; /* 'random' perturbation: KEEP !! */

for(i=0 ; i< 300 ; i++) /* run for 300 pulses ... */
{
    DoOnePulse( );
    printf("%3d> z1 (%12.5e,%12.5e) z2 :(%12.5e,%12.5e)\n",
           i,z1Re,z1Im,z2Re,z2Im);
}
return( 0 );
}

```

The function DoOnePulse( ) is the 'work-horse' of the program. It uses the two present (complex) mechanical amplitudes z1 and z2 to calculate the voltage excitation. It scales the voltage vector sum to the design average value, determines the corresponding 'Lorentz kick' for the two cavities and with it the new amplitudes z1New and z2New after oscillation during the linac repetition time T. These new variables serve as the present ones for the next pulse.

```

void DoOnePulse( void )
{
    double GRe,GIm,U1Re,U1Im,U2Re,U2Im,USumRe,USumIm,USumAbs2;
    double z1NewRe,z1NewIm,z2NewRe,z2NewIm,aux1,aux2;
    /* determine tune dependent relative voltages: */
    /* U = 1/(1 - 2*i*(xtune + Re(z)) */
    aux1 = 2.*(xtune + z1Re);
    U1Re = 1./(1. + aux1*aux1);
    U1Im = aux1/(1. + aux1*aux1);
    aux2 = 2.*(xtune + z2Re);
    U2Re = 1./(1. + aux2*aux2);
    U2Im = aux2/(1. + aux2*aux2);
    /* calculate vector sum */
    USumRe = U1Re + U2Re;
    USumIm = U1Im + U2Im;
    /* calibration constant G = 2/(U1+U2) */
    USumAbs2 = USumRe*USumRe + USumIm*USumIm;
    GRe = +2.*USumRe/USumAbs2;
    GIm = -2.*USumIm/USumAbs2;
    /* vector sum enforces sum voltage '2' : V=G*U */
    V1Re = U1Re*GRe - U1Im*GIm;
    V1Im = U1Re*GIm + U1Im*GRe;
    V2Re = U2Re*GRe - U2Im*GIm;
    V2Im = U2Re*GIm + U2Im*GRe;
    /* Lorentz kick proportional to |V|^2 */
    kick1 = kick0*(V1Re*V1Re + V1Im*V1Im);
    kick2 = kick0*(V2Re*V2Re + V2Im*V2Im);
    /* apply it */
    z1Im = z1Im - kick1;
    z2Im = z2Im - kick2;
    /* let cavities oscillate for time T: z'=z*rho */
    z1NewRe = z1Re*rhoRe - z1Im*rhoIm;
    z1NewIm = z1Im*rhoRe + z1Re*rhoIm;
    z2NewRe = z2Re*rhoRe - z2Im*rhoIm;
    z2NewIm = z2Im*rhoRe + z2Re*rhoIm;
    /* these are the input z for the next pulse */
    z1Re = z1NewRe;
    z1Im = z1NewIm;
    z2Re = z2NewRe;
}

```

```

    z2Im = z2NewIm;
        /*          and that's it for this pulse          */
}

```

---

The following two functions, call and prototype are only optional (but handy ..) **SetEquil()** finds the ('naïve') mechanical equilibrium position for both cavities **Eigenvalues()** calculates eigenvalues and predicts instability (formula (39)).

```

void SetEquil( void )
{
    /* set all mech. cavity amplitudes on equilibrium */
    double aux;
    aux = 1. + rhoRe*rhoRe + rhoIm*rhoIm - 2.*rhoRe;
    z1Re = +kick0*rhoIm/aux;
    z1Im = -kick0*(rhoRe - rhoRe*rhoRe - rhoIm*rhoIm)/aux;
    z2Re = z1Re;
    z2Im = z1Im;
    printf("z.eq (%10.7f,%10.7f) x0 %10.7f\n", z1Re, z1Im, xtune+z1Re);
}

void Eigenvalues( void )
{
    double alp, diskr, aux, xeq, x0, xi, ev1, ev2;
    aux = 1. + rhoRe*rhoRe + rhoIm*rhoIm - 2.*rhoRe;
    xeq = +kick0*rhoIm/aux;
    x0 = xtune + xeq;
    xi = 8.*kick0*x0/(1.+4.*x0*x0);
    alp = rhoRe - 0.5*xi*rhoIm;
    diskr = alp*alp - (rhoRe*rhoRe+rhoIm*rhoIm);
    if( diskr < 0. )
    {
        printf("xi %10.7f E.V. %10.7f+i*%10.7f |E.V.| %10.7f\n\n",
            xi, alp, sqrt(-diskr), rhoAbs);
    }
    else
    {
        ev1 = alp - sqrt(diskr);    ev2 = alp + sqrt(diskr);
        printf("xi %10.7f E.V.    %10.7f ,    %10.7f\n", xi, ev1, ev2);
        if(fabs(ev1) >1. || fabs(ev2) >1.) printf("[Unstable]\n");
        printf("\n");
    }
}

```

## APPENDIX D: PROGRAM OUTPUT EXAMPLES

Following two ‘runs’ with 10 MV/m and 10.01 MV/m, else identical parameter, for 2 cavities supplied by one transmitter. Shown are the two (complex) mechanical cavity amplitudes  $z_1$  and  $z_2$ . In the first run the cavities stay on the ‘naïve’ equilibrium, in the second case they behave uncontrollable after about 100 pulses.

The fate of the run can already be predicted by the absolute eigenvalue (larger/smaller 1) calculated by the formula (39) derived in this paper.

Output for the **stable** case with **E0 = 10 MV/m**  
(equilibrium start)

```
|rho| 8.95627e-01 phiDeg 480.000 xtune 1.26120 E0 10.00000
z.eq (-1.2937925,-2.0849870) x0 -0.0325925
xi 1.1683666 E.V. -0.9985057 , -0.8033480

0> z1 (-1.29379e+00,-2.08499e+00) z2 :(-1.29379e+00,-2.08499e+00)
1> z1 (-1.29379e+00,-2.08499e+00) z2 :(-1.29379e+00,-2.08499e+00)
2> z1 (-1.29379e+00,-2.08499e+00) z2 :(-1.29379e+00,-2.08499e+00)
. . . . .
297> z1 (-1.29379e+00,-2.08499e+00) z2 :(-1.29379e+00,-2.08499e+00)
298> z1 (-1.29379e+00,-2.08499e+00) z2 :(-1.29379e+00,-2.08499e+00)
299> z1 (-1.29379e+00,-2.08499e+00) z2 :(-1.29379e+00,-2.08499e+00)
```

Output for the **unstable** case with **E0 = 10.01 MV/m**  
(equilibrium start, same RF tune as before)

```
|rho| 8.95627e-01 phiDeg 480.000 xtune 1.26120 E0 10.01000
z.eq (-1.2963814,-2.0891591) x0 -0.0351814
xi 1.2628130 E.V. -1.2147940 , -0.6603158
[Unstable]

0> z1 (-1.29638e+00,-2.08916e+00) z2 :(-1.29638e+00,-2.08916e+00)
1> z1 (-1.29638e+00,-2.08916e+00) z2 :(-1.29638e+00,-2.08916e+00)
2> z1 (-1.29638e+00,-2.08916e+00) z2 :(-1.29638e+00,-2.08916e+00)
. . . . .
30> z1 (-1.29638e+00,-2.08916e+00) z2 :(-1.29638e+00,-2.08916e+00)
31> z1 (-1.29638e+00,-2.08916e+00) z2 :(-1.29638e+00,-2.08916e+00)
. . . . .
60> z1 (-1.29737e+00,-2.08889e+00) z2 :(-1.29540e+00,-2.08944e+00)
61> z1 (-1.29519e+00,-2.08950e+00) z2 :(-1.29759e+00,-2.08884e+00)

90> z1 ( 3.60853e-01,-1.27884e+01) z2 :( 5.01867e+01,-1.53643e+01)
91> z1 (-3.38633e+00,-1.58191e+00) z2 :(-1.05715e+01, 4.57987e+01)
. . . . .
120> z1 (-1.89852e+00, 3.29843e+02) z2 :(-5.92071e-01, 1.91274e+02)
121> z1 (-2.64739e+02,-1.54810e+02) z2 :(-1.57264e+02,-9.14088e+01)
. . . . .
150> z1 (-1.84068e+00, 8.12721e+01) z2 :(-1.55109e+01,-3.41352e+01)
151> z1 (-7.50880e+01,-4.52557e+01) z2 :( 3.33854e+01, 3.23397e+00)
. . . . .
180> z1 (-1.59182e+03,-9.17094e+02) z2 :(-1.26148e+03,-7.33305e+02)
181> z1 ( 1.42144e+03,-8.25566e+02) z2 :( 1.12933e+03,-6.52580e+02)
. . . . .
```

**Following a tune scan from  $x_{\text{tune}} = -6.38$  to  $x_{\text{tune}} = +3.78300$ :**  
 (equilibrium start, constant parameters except 'xtune')

```
|rho| 8.95627e-01 phiDeg 480.000 xtune -6.38000 E0 10.00000
z.eq (-1.2937925,-2.0849870) x0 -7.6737925
xi 1.1678649 E.V. -0.9964980 , -0.8049666
```

```
|rho| 8.95627e-01 phiDeg 480.000 xtune -5.00000 E0 10.00000
z.eq (-1.2937925,-2.0849870) x0 -6.2937925
xi 1.4210120 E.V. -1.4412512 , -0.5565633
[Unstable]
```

```
0> z1 (-1.29379e+00,-2.08499e+00) z2 :(-1.29379e+00,-2.08499e+00)
1> z1 (-1.29379e+00,-2.08499e+00) z2 :(-1.29379e+00,-2.08499e+00)
. . . . .
296> z1 (-1.05873e+01,-6.81706e-01) z2 :( 5.25138e+00,-7.91730e+00)
297> z1 ( 5.25138e+00,-7.91730e+00) z2 :(-1.05873e+01,-6.81706e-01)
298> z1 (-1.05873e+01,-6.81706e-01) z2 :( 5.25138e+00,-7.91730e+00)
299> z1 ( 5.25138e+00,-7.91730e+00) z2 :(-1.05873e+01,-6.81706e-01)
```

```
|rho| 8.95627e-01 phiDeg 480.000 xtune 1.26100 E0 10.00000
z.eq (-1.2937925,-2.0849870) x0 -0.0327925
xi 1.1754749 E.V. -1.0240848 , -0.7832824
[Unstable]
```

```
|rho| 8.95627e-01 phiDeg 480.000 xtune 1.26120 E0 10.00000
z.eq (-1.2937925,-2.0849870) x0 -0.0325925
xi 1.1683666 E.V. -0.9985057 , -0.8033480
```

```
|rho| 8.95627e-01 phiDeg 480.000 xtune 1.30000 E0 10.00000
z.eq (-1.2937925,-2.0849870) x0 0.0062075
xi -0.2234345 E.V. -0.3611616+i* 0.8195791 |E.V.| 0.8956269
```

```
|rho| 8.95627e-01 phiDeg 480.000 xtune 1.39420 E0 10.00000
z.eq (-1.2937925,-2.0849870) x0 0.1004075
xi -3.4745519 E.V. 0.8143801 , 0.9849794
```

```
|rho| 8.95627e-01 phiDeg 480.000 xtune 1.39440 E0 10.00000
z.eq (-1.2937925,-2.0849870) x0 0.1006075
xi -3.4809347 E.V. 0.7938211 , 1.0104891
[Unstable]
```

```
|rho| 8.95627e-01 phiDeg 480.000 xtune 1.40000 E0 10.00000
z.eq (-1.2937925,-2.0849870) x0 0.1062075
xi -3.6584014 E.V. 0.5959408 , 1.3460190
[Unstable]
```

```
0> z1 (-1.29379e+00,-2.08499e+00) z2 :(-1.29379e+00,-2.08499e+00)
1> z1 (-1.29379e+00,-2.08499e+00) z2 :(-1.29379e+00,-2.08499e+00)
. . . . .
298> z1 (-1.26567e+00,-2.03966e+00) z2 :(-1.33329e+00,-2.14864e+00)
299> z1 (-1.26567e+00,-2.03966e+00) z2 :(-1.33329e+00,-2.14864e+00)
```

```
|rho| 8.95627e-01 phiDeg 480.000 xtune 3.78000 E0 10.00000
z.eq (-1.2937925,-2.0849870) x0 2.4862075
xi -3.4792529 E.V. 0.7987419 , 1.0042639
[Unstable]
```

```
|rho| 8.95627e-01 phiDeg 480.000 xtune 3.78300 E0 10.00000
z.eq (-1.2937925,-2.0849870) x0 2.4892075
xi -3.4753851 E.V. 0.8113598 , 0.9886459
```

## REFERENCES

- [1] J. Tückmantel, ” ‘SPLinc’, A Program to Simulate SC Linac RF System with beam”, CERN-SL-Note-2000-053-HRF  
<http://sl.web.cern.ch/SL/Publications/HRF2000-053.pdf>  
The program is in principle designed for longitudinal beam dynamic simulations for a proton linac with superconducting cavities suffering microphonics and Lorentz detuning. However, it allows – intended initially only for diagnostic means – displaying the internal working of any of its transmitter-cavity ‘families’; this is possible even without executing the beam simulation.
- [2] ‘Conceptual Design of a High Intensity Superconducting H<sup>-</sup> Linac at CERN’, ed. A. Lombardi and M. Vretenar, CERN 2000-0012 (‘Yellow Report’)  
[http://preprints.cern.ch/cgi-bin/setlink?base=cernrep&categ=Yellow\\_Report&id=2000-012](http://preprints.cern.ch/cgi-bin/setlink?base=cernrep&categ=Yellow_Report&id=2000-012)
- [3] For information on TESLA scan <http://tesla.desy.de/>
- [4] Priv. comm. St. Simrock, DESY
- [5] Matthias Liepe, DESY, “Active Control of Lorentz Detuning and Microphonics”, talk at the ‘Workshop on Low Level RF Control for SC Linacs’ held at Thomas Jefferson Laboratory, Newport News, USA, 24-26 April 2001.  
<http://www.jlab.org/LLRF/Liepe.pdf>